

2.1.4. FLASK MEASUREMENTS OF METHANE

During 1993, the determination of the global distribution of atmospheric CH₄ continued at 37 sampling sites of the Carbon Cycle Division's cooperative air sampling network. The gaps in the data records (see section 2.1.2) prevent us from including annual means for shipboard samples collected in 1993. Sampling was started at three new sites during the year: Hegyhatsal, Hungary, HUN (March), Wendover, Utah, UTA (May), and Dwejra Point, Gozo, Malta, GOZ (October). Two of the sites are continental (HUN and UTA), and they should provide interesting new data to complement the other sites in the CMDL predominantly ocean-based network. Provisional annual mean values for 1993 are given in Table 2.4.

One of the best known constraints on understanding the global atmospheric CH₄ budget is the rate of growth. Because of the importance of CH₄ as a greenhouse gas, variations in the trend have been newsworthy, especially during 1992 to 1993 when dramatic changes in growth rate were observed [Steele *et al.*, 1992; Dlugokencky *et al.*, 1994a, b]. The CH₄ growth rates for the northern and southern hemispheres determined from the smoothed CMDL flask sample data are shown in Figure 2.11. In both hemispheres, a long-term decrease in the rate of increase was observed. In addition, significant interannual variations were also present.

In the southern hemisphere, there was a large increase in the growth rate during 1988-1989. Such changes can be explored quantitatively using mass balance equations. For the southern hemisphere, the rate of increase in CH₄ is given by

$$dS/dt = Q_s + f(N-S) - kS \quad (2)$$

where S and N are the burdens for the southern and northern hemispheres, Q_s is the CH₄ source strength in the southern hemisphere, f is the inverse of interhemispheric exchange time (~1 yr⁻¹), and k is the inverse of the methane lifetime (~0.1 yr⁻¹). The second derivative is:

$$d^2S/dt^2 = df/dt(N-S) + fd(N-S)/dt + dQ_s/dt - kdS/dt - Sdk/dt. \quad (3)$$

Except for the first term on the right-hand side, all of the terms in eq. 3 can be estimated from the measurement data, and d²S/dt² is determined by taking the derivative of the growth rate curve in Figures 2.11 and 2.12. In 1988-1989, it was ~10 ppb yr⁻² or 14 Tg yr⁻². The difference in hemispheric burdens is determined as the difference between the annual means for each hemisphere, which is about 90 ppb or 125 Tg. It was assumed that this difference does not vary with time, although interannual variations in this parameter have been observed [Steele *et al.*, 1992]. The last three terms on the right-hand side of eq. 2 were interpreted as the fall off in the southern hemisphere growth rate, determined as twice

TABLE 2.4. Provisional 1993 Annual Mean CH₄ Mixing Ratios From the Flask Network Sites

Code	Station	CH ₄ (ppm)
ALT	Alert, N.W.T., Canada	1799.1
ASC	Ascension Island	1678.2
BAL	Baltic Sea	1810.3
BME	Bermuda (east coast)	1773.6
BMW	Bermuda (west coast)	1772.8
BRW	Barrow, Alaska	1807.0
CBA	Cold Bay, Alaska	1792.9
CGO	Cape Grim, Tasmania	1667.6
CHR	Christmas Island	1693.3
CMO	Cape Meares, Oregon	1782.1
GMI	Guam, Mariana Islands	1723.6
GOZ	Dwejra Point, Gozo, Malta	[]
HUN	Hegyhatsal, Hungary	[]
ICE	Vestmannaeyjar, Iceland	1793.2
ITN	WITN, Grifton, N. Carolina	1810.7
IZO	Izaña Observatory, Tenerife	1754.1
HBA	Halley Bay, Antarctica	[]
KEY	Key Biscayne, Florida	1750.9
KUM	Cape Kumukahi, Hawaii	1745.5
MBC	Mould Bay, Canada	1803.2
MHT	Mace Head, Ireland	1787.3
MID	Midway Island	1760.0
MLO	Mauna Loa, Hawaii	1727.1
NWR	Niwot Ridge, Colorado	1760.6
PSA	Palmer Station, Antarctica	1668.3
QPC	Qinghai Province, China	1764.7
RPB	Ragged Point, Barbados	1733.7
SEY	Mahé Island, Seychelles	1687.2
SGI	South Georgia Island	[]
SHM	Shemya Island, Alaska	1794.6
SMO	American Samoa	1672.5
SPO	South Pole, Antarctica	1666.7
STM	Ocean Station M	1796.6
SYO	Syowa Station, Antarctica	1677.2
TAP	Tae-ahn Peninsula, S. Korea	1833.9
UTA	Wendover, Utah	[]
UUM	Ulaan Uul, Mongolia	1797.0

Square brackets indicate insufficient data to calculate annual mean.

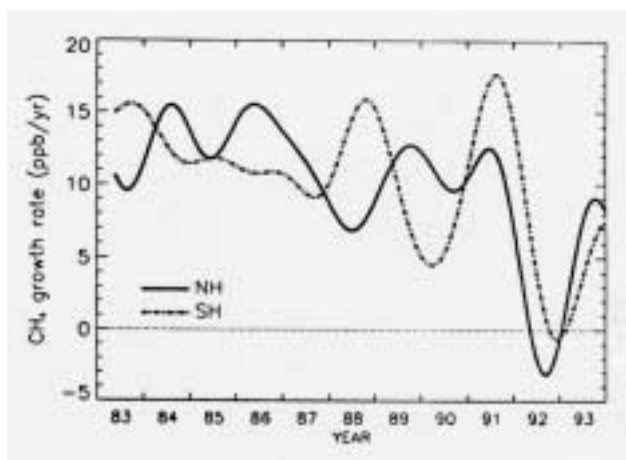


Fig. 2.11. Instantaneous growth rate curves averaged over the northern (solid line) and southern hemispheres (dashed line).

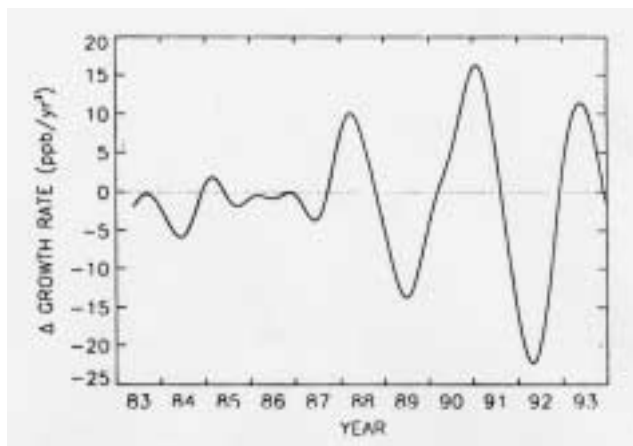


Fig. 2.12. Derivative of the southern hemisphere growth rate curve shown in Figure 2.11 (dashed line). The positive deviations are used to evaluate the left hand side of equation 3 (section 2.1.4).

the coefficient a_3 from a fit of eq. 1 to the smoothed southern hemisphere data. This gives -0.5 ppb yr^{-2} or -0.7 Tg yr^{-2} . Filling in these values in eq. 3 suggests that an enhancement by about 12% over average interhemispheric transport is necessary to explain the observation. *Steele et al.* [1992] suggested that increased interhemispheric transport occurred in 1988-1989 because of a La Niña event. La Niña events are characterized by relatively cold surface temperatures in the equatorial Pacific and positive westerly wind anomalies at 200 mbar in the central, equatorial Pacific. Such conditions may be conducive to enhanced transport of trace gases between the hemispheres. Since CH_4 mixing ratios are always greater in the northern hemisphere than the southern hemisphere, such increased transport would lead to an apparent increase in the growth rate in the southern hemisphere. This hypothesis is supported by an observed simultaneous decrease in the growth rate in the northern hemisphere by a similar amount.

The effects of a change in interhemispheric transport on the hemispheric growth rates were investigated with a 2-box model, with one box for each hemisphere. In the model, sources and sinks were constant, but the interhemispheric exchange term was increased by 10% during 1988 and then returned to normal in 1989. The growth rate for the model result is shown in Figure 2.13. The apparent decrease in growth rate in the year following the increased interhemispheric exchange occurs in the model result, and the observation, as the trend, comes back to its average value.

During 1991, another large oscillation in the growth rate was observed, but a La Niña was not. Enhanced interhemispheric transport may have resulted because of the effects of aerosol injected into the atmosphere by the eruption of Mount Pinatubo [*Pitari, 1993*]. The change in f required to explain the measurements was about 18%. A corresponding change in growth rate in the northern hemisphere was not observed, suggesting that if interhemispheric exchange was responsible for the change in southern hemispheric growth rate at that time, there must have been a significant change in northern hemisphere sources or sinks.

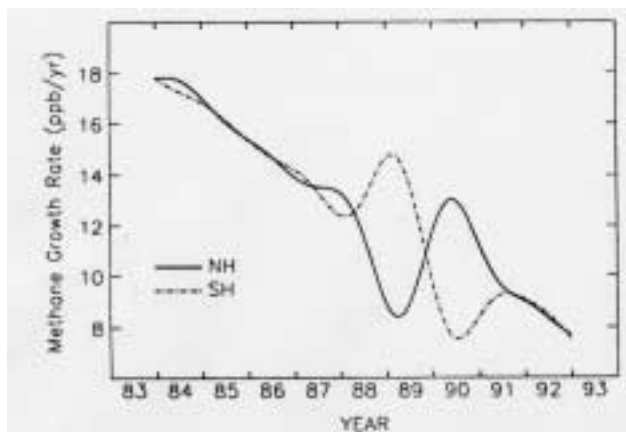


Fig 2.13. Growth rate curves determined from a 2-box model where interhemispheric transport was increased by 10% during 1988 and then returned to normal in 1989. All other source and sink terms in the model remained constant.

During 1992 and 1993, the CH_4 growth rate in the southern hemisphere decreased dramatically. The increase in CH_4 during 1992 was $(5.0 \pm 0.8) \text{ ppb}$ and $(3.6 \pm 1.0) \text{ ppb}$ during 1993. These values compare with a trend of $(10.6 \pm 0.1) \text{ ppb yr}^{-1}$ averaged over the full measurement period (1983-1993). The cause of this decrease is still unknown. In part it is a response to the large increase in growth rate just prior to this, but CH_4 stable isotope data [*Lowe et al., 1994*] indicate that decreased emissions of fossil CH_4 in the northern hemisphere [*Dlugokencky et al., 1994a*] and decreased biomass burning in the tropics may have played a significant role.